Stem Cell Reports
Article

ISSCR

OPEN ACCESS

Enhancement of Sensitivity to Chemo/Radiation Therapy by Using miR-15b against *DCLK1* in Colorectal Cancer

Dengbo Ji,[1,8] Tiancheng Zhan,[1,8] Ming Li,[1,8] Yunfeng Yao,[1] Jinying Jia,[1] Haizhao Yi,[1] Meng Qiao,[1] Jinhong Xia,[1] Zhiqian Zhang,[2] Huirong Ding,[3] Can Song,[4,5] Yong Han,[6] and Jin Gu[1,5,7,*]

[1]Key Laboratory of Carcinogenesis and Translational Research, Ministry of Education, Department of Gastrointestinal Surgery III, Peking University Cancer Hospital & Institute, No. 52 Fucheng Road, Haidian District, Beijing 100142, China
[2]Department of Cell Biology, Peking University Cancer Hospital & Institute, No. 52 Fucheng Road, Haidian District, Beijing 100142, China
[3]Central Laboratory, Peking University Cancer Hospital & Institute, No. 52 Fucheng Road, Haidian District, Beijing 100142, China
[4]School of Life Sciences, Tsinghua University, Beijing 100084, China
[5]Peking-Tsinghua Center for Life Sciences, Beijing 100084, China
[6]Department of Pathology, Zhejiang Provincial People's Hospital, Hangzhou, Zhejiang 310014, China
[7]Peking University S.G. Hospital, Beijing 100144, China
[8]Co-first author
*Correspondence: zlguj@bjmu.edu.cn
https://doi.org/10.1016/j.stemcr.2018.10.015

SUMMARY

Chemo-/radiotherapy resistance is the main cause accounting for most treatment failure in colorectal cancer (CRC). Tumor-initiating cells (TICs) are the culprit leading to CRC chemo-/radiotherapy resistance. The underlying regulation mechanism of TICs in CRC remains unclear. Here we discovered that miR-15b expression positively correlated with therapeutic outcome in CRC. Expression of miR-15b in pretreatment biopsy tissue samples predicted tumor regression grade (TRG) in rectal cancer patients after receiving neoadjuvant radiotherapy (nRT). Expression of miR-15b in post-nRT tissue samples was associated with therapeutic outcome. *DCLK1* was identified as the direct target gene for miR-15b and its suppression was associated with self-renewal and tumorigenic properties of DCLK1+ TICs. We identified B lymphoma Mo-MLV insertion region l homolog (BMI1) as a downstream target regulated by miR-15b/DCLK1 signaling. Thus, miR-15b may serve as a valuable marker for prognosis and therapeutic outcome prediction. DCLK1 could be a potential therapeutic target to overcome chemo-/radioresistance in CRC.

INTRODUCTION

Up to 90% of patients with colorectal cancer (CRC) can be cured by surgery if the disease is detected at a very early stage. However, a high proportion of patients are diagnosed at advanced stages, resulting in poor survival (Siegel et al., 2014). Chemo-/radiotherapy may have significant therapeutic value for those patients, although the efficacy of chemo-/radiotherapy varies among individual patients due to differences in the molecular composition of tumors and individual genomic backgrounds. Unfortunately, our knowledge to identify patients who are more likely to benefit from targeted adjuvant chemotherapy and/or neoadjuvant chemo-/radiotherapy is very limited (Aklilu and Eng, 2011; Gangadhar and Schilsky, 2010; Van Schaeybroeck et al., 2011). There is, hence, an urgent need to find useful molecular biomarker(s) to stratify patients with respect to prognosis and response to therapy.

Previous studies have reported that tumor chemo-/radiotherapy resistance is associated with characteristics of tumor stem cells (Avoranta et al., 2013; Cho et al., 2012). Although tumor-initiating cells (TICs) account for only a small proportion of tumor tissue, they maintain tumor growth and differentiation potential (Eaton et al., 2010; Kuhn and Tuan, 2010). TICs have many unique features, such as self-renewal and heterotrophic differentiation potential, possession of a variety of drug efflux pumps, and strong DNA repairing ability. These features may be associated with the tolerance of tumors against existing chemo-/radiotherapy. Existence of TICs has been confirmed in the majority of cancer types. During prolonged conventional chemo-/radiotherapy, these tumors usually show enrichment of TICs, which induce resistance to the treatment. This suggests that blocking the function of TICs is critical to eliminating tumor cells. Therefore, targeted therapy against TICs is promising for preventing tumorigenesis, metastasis, and resistance to chemo-/radiotherapy.

Mounting evidence has shown that microRNAs (miRs) are often dysregulated and may serve as either tumor suppressors or oncogenes in multiple cancers (Calin and Croce, 2006; Grady and Tewari, 2010). These miRs have emerged as potential prognostic and/or therapeutic biomarkers as well as therapeutic targets. Several studies have demonstrated that miRs play important roles in chemo-/radioresistance in various cancers, and their expression in TICs is related to tumorigenicity and therapeutic resistance (Asuthkar et al., 2012; Bitarte et al., 2011; Song et al., 2009). In CRC, miR-21 and miR-320 have already been reported to be implicated in chemo-/radioresistance (Lopes-Ramos et al., 2014; Wan et al., 2015).

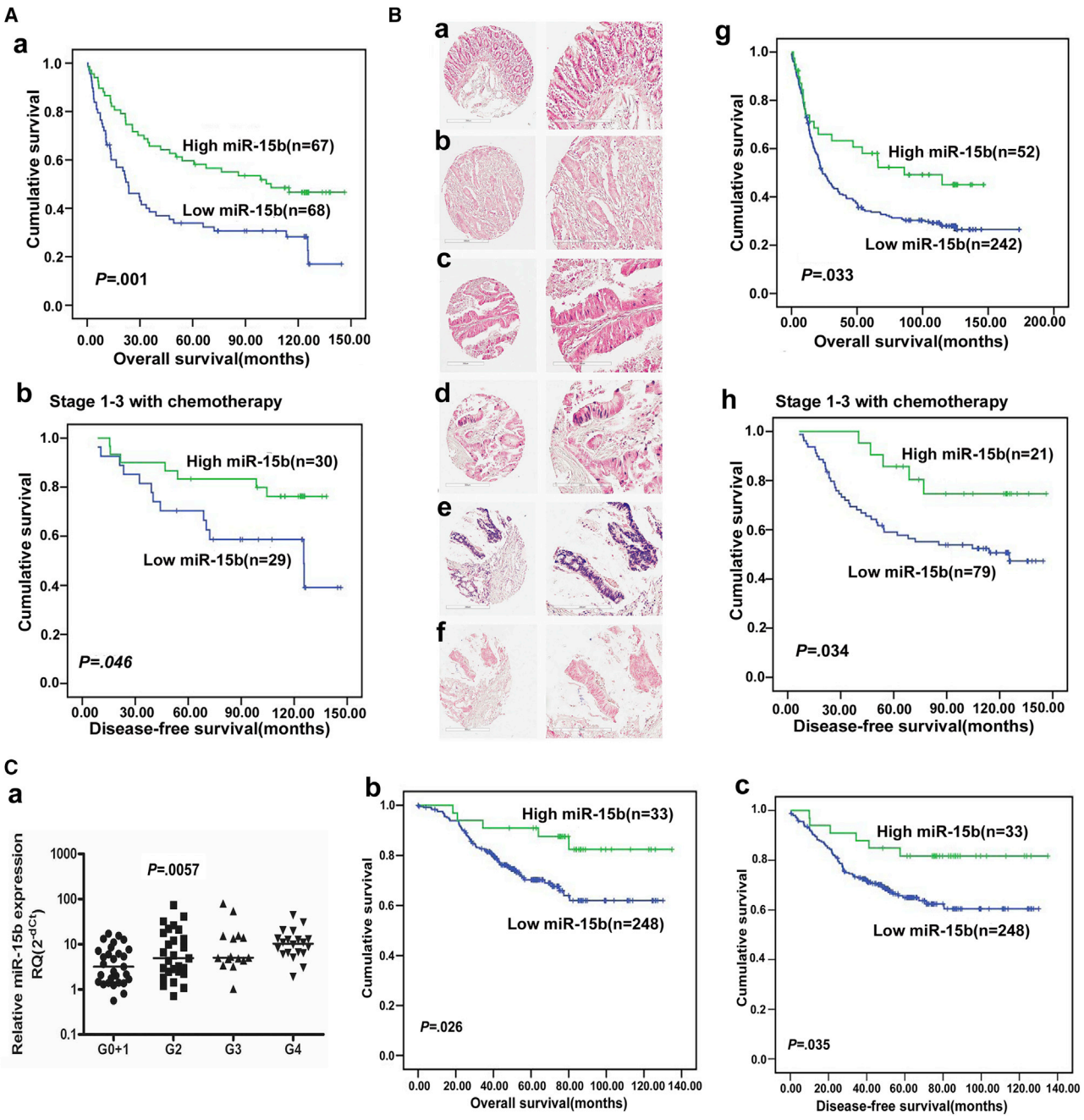

Figure 1. Association between miR-15b Expression and Prognosis after Chemo-/Radiotherapy

(A) qRT-PCR results in cohort 1: (a) Kaplan-Meier analysis of the correlation between miR-15b expression levels and OS; (b) association between miR-15b expression and chemotherapy outcome in patients with TNM stage I–III CRC.

(B) Expression of miR-15b in colorectal epithelial cells using ISH analysis. The positive staining of epithelium cells was expressed as blue-violet, and the representative results are shown. (a) Expression in most normal colorectal mucosa; (b) negative expression in some CRC tissues; (c) weak positive (+); (d) strong positive (2+); (e) the nuclear expression of U6 (positive control); (f) scrambled oligonucleotide probe (negative control). Scale bars, 300 μm (left), 200 μm (right). (g) Kaplan-Meier analysis of the correlation between miR-15b expression levels and OS in cohort 2 group. (h) Kaplan-Meier analysis in TNM stage I–III CRC with chemotherapy.

(C) Expression of miR-15b in pre and post-nRT rectal cancer tissue samples and therapeutic outcomes from neoadjuvant radiotherapy. (a) Association between miR-15b expression in pretreatment biopsy tissue samples and TRG in 92 LARC patients after nRT as determined by qRT-PCR. (b and c) Kaplan-Meier analysis of post-nRT rectal patients in cohort 3.

(legend continued on next page)

In our previous work, we compared the differential microRNA profiling between CRC tissues with synchronous liver metastases and without liver metastases (follow up >6 years) by microRNA microarray profiling. miR-15b was shown to be highly expressed in CRC without liver metastases, indicating that miR-15b might be associated with better prognosis of CRC (Ji et al., 2014). miR-15b was reported to be a tumor suppressor and negatively correlated with tumor recurrence (Chung et al., 2010; Sun et al., 2015). Overexpression of miR-15b could enhance the sensitivity of colon cancer cells to 5-fluorouracil (5-FU) by promoting apoptosis via the nuclear factor κB/XIAP axis (Zhao et al., 2017). In this study, we further investigated the role of miR-15b as a predictive biomarker for the efficacy of adjuvant chemotherapy and neoadjuvant radiotherapy in CRC patients. Our results indicate that miR-15b overexpression suppresses the self-renewal and tumorigenic properties of TICs and subsequently restores chemo-/radiosensitivity by targeting *DCLK1*.

RESULTS

Expression of miR-15b and Therapeutic Outcome of Adjuvant Chemotherapy

We performed qRT-PCR analyses in 135 paired CRC and normal tissues (cohort 1). Our findings showed that there was a significant reduction in miR-15b expression in tumor tissues compared with matched adjacent normal tissues (n = 135, $p < 0.0001$). Decreased miR-15b expression significantly correlated with advanced TNM stages and liver metastases (Figures S1A–S1C). Low miR-15b expression (below the median value in this patient cohort) was associated with poor overall survival (OS) (n = 135, p = 0.001, Figure 1A, a) and disease-free survival (DFS) (n = 72, p = 0.049, Figure S1D). We analyzed associations between miR-15b expression and therapeutic outcomes in patients with stage I, II, and III CRC treated with adjuvant chemotherapy. The chemotherapy regimens were primarily fluorouracil-based, with or without leucovorin, levamisole, or oxaliplatin. The patients who received adjuvant chemotherapy with a low miR-15b expression were associated with a poor therapeutic outcome (n = 59, p = 0.046, Kaplan-Meier log rank, Figure 1A, b) in cohort 1 group.

These results were also observed in cohort 2 (n = 294) by *in situ* hybridization (ISH) (Figure 1B). Reduced miR-15b expression (negative expression) in tumor tissue was significantly associated with shorter OS (n = 294, p = 0.033, Log rank test, Figure 1B, g). Low miR-15b expression was associated with a worse prognosis in patients with stage I- III CRC cancer treated with adjuvant chemotherapy (n = 100, p = 0.034, Figure 1B, h). Cox regression analysis further confirmed that low miR-15b expression was an independent risk factor for poor survival (hazard ratio [HR] 0.344; 95% confidence interval [CI] 0.198–0.597; $p < 0.0001$, Table 1).

The correlation between miR-15b expression and OS was also confirmed in The Cancer Genome Atlas (TCGA) CRC dataset. There are 579 subjects that have both survival and microRNA expression data. Among of these patients, 28 patients with clear information indicating radiotherapy were excluded. The patients were separated into two groups according to the microRNA expression median. High miR-15b expression was associated with better OS (n = 551, p = 0.047, Figure S1E).

Expression of miR-15b Predicts Postoperative Tumor Regression Grade

Expression of miR-15b in pretreatment biopsy tissue samples was assayed by qRT-PCR in 92 locally advanced rectal cancer (LARC) patients (from cohort 3) who received neoadjuvant radiotherapy. Expression of miR-15b was significantly correlated with tumor regression grade (TRG) (p = 0.0057). Patients with high miR-15b expression were more likely to achieve pathological response after neoadjuvant radiation treatment. The intensity of miR-15b expression in complete responders (TRG 4) was significantly higher (p = 0.0005, Figure 1C, a) than the non-responders (TRG 0 + 1).

Clinical Implication of miR-15b Expression after Neoadjuvant Radiotherapy

Using ISH, miR-15b expression in post-neoadjuvant radiotherapy rectal cancer tissues was evaluated. miR-15b positive expression was defined as high expression and positive correlation with DFS and OS was found (cohort 3, n = 296, p = 0.026, p = 0.035, respectively, Kaplan-Meier plot in Figures 1C, b and c, and S2A). Cox regression analysis also identified low levels of miR-15b as an independent risk factor for poor DFS in post-neoadjuvant radiotherapy LARC patients (HR 0.41, 95% CI 0.175 to 0.957, p = 0.039, Table 2).

These discoveries were further validated in cohort 4 (n = 70) by qRT-PCR (Figure S2B, Table 2).

In (A, a and b), the patients were divided into two groups according to the median expression value. Below the median value was defined as low expression, above the median value was defined as high expression. In (B, g and h), and (C, b and c), miR-15b positive expression was defined as high expression; miR-15b negative expression was defined as low expression. $p \leq 0.05$ was considered statistically significant. See also Figures S1 and S2.

Table 1. Univariate and Multivariate Cox Regression Analysis of miR-15b Expression Levels and Overall Cancer Survival in Subjects with Colorectal Cancer

	Cohort 1				Cohort 2			
	Univariate Analysis		Multivariate Analysis		Univariate Analysis		Multivariate Analysis	
Characteristic	HR (95% CI)	p Value	HR (95% CI)	p Value	HR (95% CI)	p Value	HR (95% CI)	p Value
miR-15b expression (high/low)	0.495 (0.32–0.766)	0.002	0.344 (0.198–0.597)	0.000	0.606 (0.38–0.966)	0.035	0.597 (0.361–0.988)	0.045
Gender (male/female)	0.801 (0.518–1.241)	0.321	0.841 (0. 498–1.419)	0.516	0.887 (0.658–1.194)	0.428	1.16 (0.851–1.58)	0.349
Age (≤60 years [median]/>60 years)	1.084 (0.705–1.665)	0.714	1.267 (0.76–2.111)	0.365	1.107 (0.824–1.488)	0.498	1.342 (0.989–1.822)	0.059
Venous invasion (positive/negative)	2.256 (1.459–3.49)	0.000	1.489 (0.836–2.652)	0.176	2.141 (1.586–2.89)	0.000	1.388 (1.003–1.922)	0.048
TNM stage (I-II/III-IV)	5.101 (2.806–9.273)	0.000	9.679 (3.544–26.432)	0.000	5.122 (3.339–7.855)	0.000	6.576 (3.615–11.965)	0.000
Histological type (adenocarcinoma/ mucinous adenocarcinoma)	0.895 (0.327–2.447)	0.829	0.705 (0.224–2.219)	0.55	0.947 (0.466–1.925)	0.881	0.636 (0.25–1.617)	0.342
Lymph node metastasis (positive/negative)	3.109 (1.888–5.121)	0.000	2.809 (1.214–6.54)	0.016	2.802 (2.0–3.926)	0.000	1.49 (0.2–2.415)	0.105
Differentiation (poor/well)	0.691 (0.421–1.136)	0.145	0.507 (0.271–0.95)	0.034	0.867 (0.763–0.985)	0.029	0.874 (0.714–1.071)	0.195
Tumor location (colon/rectum)	1.269 (0.752–2.143)	0.373	1.322 (0.754–2.317)	0.331	0.88 (0.652–1.186)	0.4	0.932 (0.679–1.28)	0.665

miR-15b Enhances Sensitivity of CRC Cells to Chemo-/Radiotherapy

We investigated whether miR-15b expression regulates CRC chemo-/radiosensitivity. We detected miR-15b overexpression increased radiosensitivity and chemosensitivity to 5-FU in CRC cells (Figures 2A and 2C). A dimly expression of miR-15b was detected in 5-FU or radioresistant HCT8 cells (HCT8 5-FU and HCT8-48Gy), and highly expressed in HCT8 cells (Figure 2B). Furthermore, miR-15b overexpression could restore chemo-/radiosensitivity in 5-FU or radioresistant CRC cells (Figures 2C, c, and 2A, e).

The inhibitory effects of miR-15b on tumor cell proliferation, invasion, and metastasis *in vitro* and *in vivo* are demonstrated in Figure S3.

Induction of lentivirus carrying miR-15b precursor repressed *in vitro* cell growth (Figure S3A, a), invasion, and migration (Figure S3C, a and c) of Lovo cells. Induction of lentivirus carrying a miRZip anti-miR-15b construct induced HT29 cell growth (Figure S3A, b), invasion, and migration (Figure S3C, b and d). *In vivo* experiments in NOD SCID (NOD.CB17-prkdcscid/NcrCrl) mice demonstrated that miR-15b inhibited tumor cell growth as shown by reduced tumor weight, miR-15b also inhibited tumor cell metastasis to the lung (Figures S3B and S3D).

DCLK1 Is a Direct Target Gene of miR-15b and Its Expression Negatively Correlated with Prognosis of CRC

Through an integrated analysis of software predictions, expression correlation, and functional studies, *DCLK1* was identified as a functional downstream target of miR-15b (Figure 3A). The 3′-UTR of *DCLK1* mRNA contains two putative binding sites (833–839 nucleotides [nt] and 851–858 nt) for the seed region of miR-15b (Figure 3A, a). Increased expression of miR-15b upon infection of miR-15b mimics significantly suppressed activity of the luciferase reporter containing wild-type *DCLK1* 3′-UTRs (45% inhibition compared with control, $p < 0.01$). The suppression was abrogated when either target site 1 or 2 was mutated (mutant 1 and mutant 2, inhibition only 27% or 10% as compared to 45%). Once both miR-15b target sites

Table 2. Univariate and Multivariate Cox Regression Analysis of miR-15b Expression Levels and Disease-Free Survival in Post-nRT Locally Advanced Rectal Cancer

	Cohort 3				Cohort 4			
	Univariate Analysis		Multivariate Analysis		Univariate Analysis		Multivariate Analysis	
Characteristic	HR (95% CI)	p Value	HR (95% CI)	p Value	HR (95% CI)	p Value	HR (95% CI)	p Value
miR-15b expression (high/low)	0.42 (0.181–0.973)	0.043	0.41 (0.175–0.957)	0.039	0.456 (0.218–0.951)	0.036	0.284 (0.115–0.702)	0.006
Gender (male/female)	0.827 (0.513–1.334)	0.436	0.844 (0.511–1.393)	0.507	1.06 (0.526–2.133)	0.871	1.626 (0.876–3.91)	0.278
Age (≤60 years [median]/ >60 years)	0.898 (0.561–1.439)	0.656	1.052 (0.624–1.773)	0.85	0.943 (0.466–1.911)	0.872	1.517 (0.681–3.378)	0.308
Venous invasion (positive/ negative)	0.65 (0.37–1.142)	0.134	0.797 (0.432–1.47)	0.467	1.696 (0.516–5.568)	0.384	3.243 (0.852–12.34)	0.084
Post-treatment T stage (ypT0-2/ypT3-4)	2.245 (1.303–3.87)	0.004	1.537 (0.818–2.887)	0.182	12.128 (1.654–88.943)	0.014	11.064 (1.395–88.735)	0.023
Post-treatment N stage (ypN0/ ypN1-2)	2.557 (1.594–4.1)	0.000	2.264 (1.299–3.944)	0.004	2.019 (0.995–4.096)	0.052	2.981 (1.287–6.903)	0.011
Differentiation (poor/well)	1.876 (1.174–2.998)	0.009	1.412 (0.828–2.409)	0.205	4.41 (2.14–9.088)	0.000	2.897 (1.296–6.477)	0.01
Tumor regression grade (0-2/3-4)	0.759 (0.449–1.282)	0.303	0.545 (0.312–0.953)	0.033	0.619 (0.297–1.291)	0.201	0.385 (0.156–0.951)	0.039

were mutated (mutant 1 + 2), this suppressive effect was completely abolished (Figure 3A, b).

DCLK1 protein and mRNA levels were substantially suppressed in miR-15b overexpressing Lovo cells as compared with control cells (Figure 3A, c and d).

DCLK1 mRNA levels were negatively correlated with miR-15b across CRC cell lines ($p = 0.015$, Pearson correlation = −0.81, Figure 3A, e) and primary tissues (Cohort1, $p = 0.011$, Pearson correlation = −0.23; Figure 3A, f). The TCGA dataset was examined for correlation of miR-15b and *DCLK1* expression, which exhibited an inverse correlation ($p = 0.015$, Pearson correlation = −0.303, Figure 3A, g).

To investigate whether *DCLK1* expression correlates with prognosis of CRC patients, we performed ISH and qRT-PCR analyses in cohorts 2 and 3 and 4. For stage I–III CRC patients in cohort 2, RNAscope results showed that high *DCLK1* was associated with a shorter DFS, though with weak statistical significance (n = 118, $p = 0.06$, Kaplan-Meier plot in Figure 3B, a–f). High *DCLK1* expression was associated with a worse prognosis in patients with stage II cancer alone (n = 56, $p = 0.034$, Kaplan-Meier plot in Figure 3B, g). High *DCLK1* expression was associated with a poor therapeutic outcome in stage I-III CRC patients (n = 90) or stage II cancer (n = 38) alone treated with adjuvant chemotherapy ($p = 0.048$, $p = 0.048$, respectively, Figure 3B, h and i).

DCLK1 expression was associated with resistance to radiotherapy. *DCLK1* expression in non-responders (TRG 0 + 1) was significantly higher ($p = 0.023$) than complete responders (TRG 4) (n = 92, cohort 3, Figure 3C, c). Radiotherapy can induce enrichment of the DCLK1+ cells in rectal cancer tissues. An elevated expression in post-treatment tumor tissue was detected compared with pretreatment rectal cancer biopsies (Figure 3C, a and b). *DCLK1* expression in post-neoadjuvant radiotherapy tissue was inversely correlated to DFS (n = 70, cohort 4, $p = 0.023$, Kaplan-Meier analysis in Figure 3C, d).

DCLK1 Expression Drives the TIC Phenotype and Chemo/Radiotherapy Resistance

To assess a potential role for DCLK1 in tumor initiation, the DCLK1+ and DCLK1− cells were separated by using fluorescence-activated cell sorting (FACS) from CRC cell lines and primary CRC tissues to assay their self-renewal

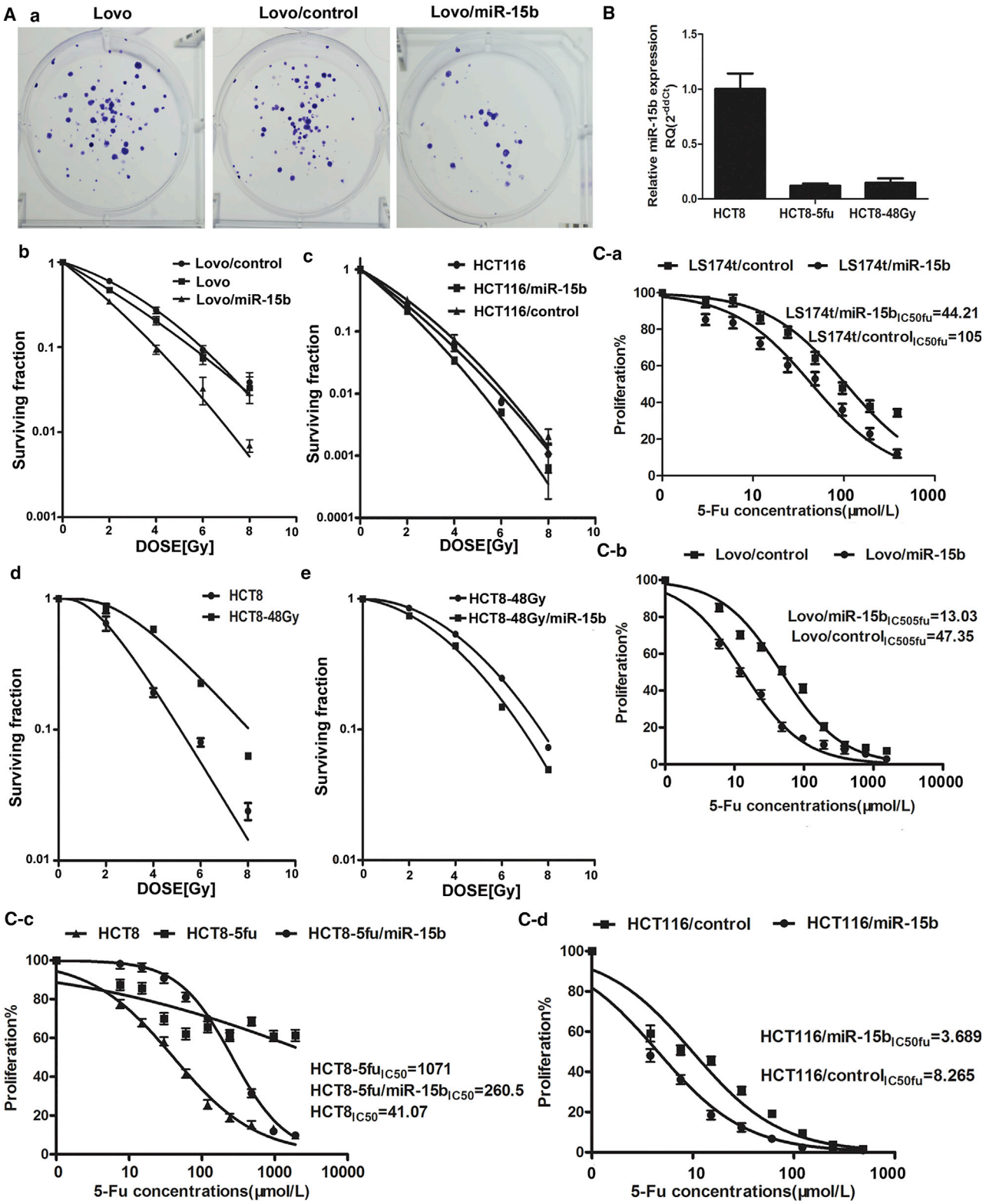

Figure 2. Expression of miR-15b Enhances *In Vitro* Chemo-/Radiosensitivity of CRC Cells

(A) The clonogenic survival of miR-15b-overexpressing CRC cells after irradiation with 2–8 Gy was compared with control cells. (a) Representative photographs of clonogenic assays. Colony formation assay of lovo versus lovo/miR-15b (b), HCT116 vs HCT116/miR-15b

(legend continued on next page)

and tumorigenic properties. Purified DCLK1+ but not DCLK1− cells were able to form compact tumor spheres and possess *in vitro* and *in vivo* self-renewal capability (Figure 4A). The expression level of DCLK1 in sorted DCLK1+ cells was higher than in DCLK1− cells (Figures S4A and S4B). Morphology of the tumor formed from the DCLK1+ cells is indistinguishable from their parent cells (Figure S4C).

The character of radioresistance was tested with the DCLK1+ and parental CRC cell lines using clonogenic assay. The DCLK1+ cells showed a significant decrease of radiosensitivity compared with the parental cells (Figure 4B, a). Furthermore, we examined the chemoresistance character of DCLK1+ and parental CRC cell lines to 5-FU. Purified DCLK1+ cells from various CRC cell lines and primary CRC tissues showed a remarkable increase in resistance to 5-FU compared with the controls, as determined by the 5-FU half maximal inhibitory concentration (IC_{50}) (Figure 4B, b–d).

The effects of chemo-/radiotherapy on the proportion of DCLK1+ cells in different CRC cell lines before and after radio- or chemotherapy were examined by FACS. The proportion of DCLK1+ cells was 9.9-fold higher in radioresistant HCT8-48Gy cell line as compared with radiosensitive controls (16.3% versus 1.65%). Similar results were observed between 5-FU resistant HCT8-5-Fu cell line and controls (14.8% versus 1.65%). Consistently, the results were confirmed by qRT-PCR. Tests on other CRC cell lines, such as HCT116 and Lovo, showed increased proportion of DCLK1+ cells following 4Gy radiotherapy (HCT116, from 2.87% to 8.29%; Lovo, from 1.41% to 2.91%) (Figure 4C).

To test for differences among DCLK1 and the other CRC TIC markers, CD44 and CD133, the tumor-forming ability of different fractions of HCT116 and Lovo cells were compared. The results showed that DCLK1 was the most robust marker for enriching the CRC TIC subpopulation, compared with CD133 and CD44, allowing us to reliably enrich CRC TICs by nearly 900-fold/300-fold, respectively (Figures 4D and S5A).

Expression of miR-15b Reverses Self-Renewal, Tumorigenicity, and Chemo/Radioresistance in DCLK1+ CRC TICs

To validate if miR-15b is involved in the regulation of DCLK1+ in CRC TICs, its expression in DCLK1+ and DCLK1− subsets was determined using qRT-PCR. The results showed that miR-15b was remarkably downregulated in DCLK1+ subsets in a variety of CRC cell lines and primary tissues compared with their DCLK1- counterparts (Figure 5A).

Overexpressed miR-15b in FACS-purified DCLK1+ TICs and its effects on the self-renewal capability of the TICs was further examined. Overexpression of miR-15b led to a remarkable inhibition of spheroid formation of DCLK1+ cells (Figure 5B). To test if miR-15b expression could modulate the chemo-/radioresistance in the DCLK1+ TICs, the miR-15b overexpressing cells were exposed to either radiation or 5-FU existing environment as described above. A significant decrease of the resistance to radiation and 5-FU was observed comparing with the parental or control cells (Figure 5D).

Compared with the control lentivirus-infected cells, tumorigenicity of DCLK1+ TICs *in vivo* was significantly suppressed by miR-15b overexpression (Figure 5C).

On the contrary, reducing miR-15b by lentiviral knockdown in DCLK1- TICs (ZIP miR-15b) yielded an opposing effect, leading to an increased tumor spheroid growth *in vitro* and enhanced ability to form tumors *in vivo* as compared with DCLK1- TICs transduced with antisense controls (ZIP CTRL) (Figures 5B and 5C).

Identification of BMI1 as a Potential Downstream Target of the miR-15b-DCLK1 Signaling Pathway

To probe the miR-15b-DCLK1-associated pathways on an unbiased basis, Gene Set Enrichment Analysis (GSEA) using high-throughput RNA-sequencing data of the TCGA database was performed. Among all the 189 predefined "oncogenic signature" gene sets, the *BMI1* pathway had the strongest association with *DCLK1* expression (Figure 5E, a). *BMI1* expression was positively correlated with *DCLK1* (Pearson correlation = 0.306, p = 0.0025) and negatively correlated with miR-15b (Pearson correlation = −0.369, p = 0.011) (Figure 5E, b and c).

The effect of miR-15b on BMI1 expression in the DCLK1+ TICs in HCT116 and Lovo cells was further examined and the result revealed that miR-15b overexpression downregulated BMI1 expression (Figure 5F, a).

The proteomic interactions of DCLK1 through the IntAact database were studied and that MYC was predicted to interact with DCLK1. BMI1 was previously reported to

(c), HCT8 versus HCT8-48Gy (d), HCT8-48Gy vs HCT8-48Gy/miR-15b (e). The radiation survival curves indicate the mean inactivation dose of CRC cells. Radiation enhancement (ER) was calculated as the ratio of the mean inactivation dose for miR-15b-overexpressing cells to control cells (ER = 1). Data are from the mean of three independent experiments ± SE.

(B) miR-15b expression in HCT8, HCT8-5fu, and HCT8-48Gy cell lines. Data are from the mean of three independent experiments ± SE.

(C) The IC_{50} of 5-FU in control or miR-15b-overexpressing CRC cells, LS174t (a), lovo (b), HCT8-5fu (c), HCT116 (d).

Data are from the mean of three independent experiments ± SE. See also Figure S3.

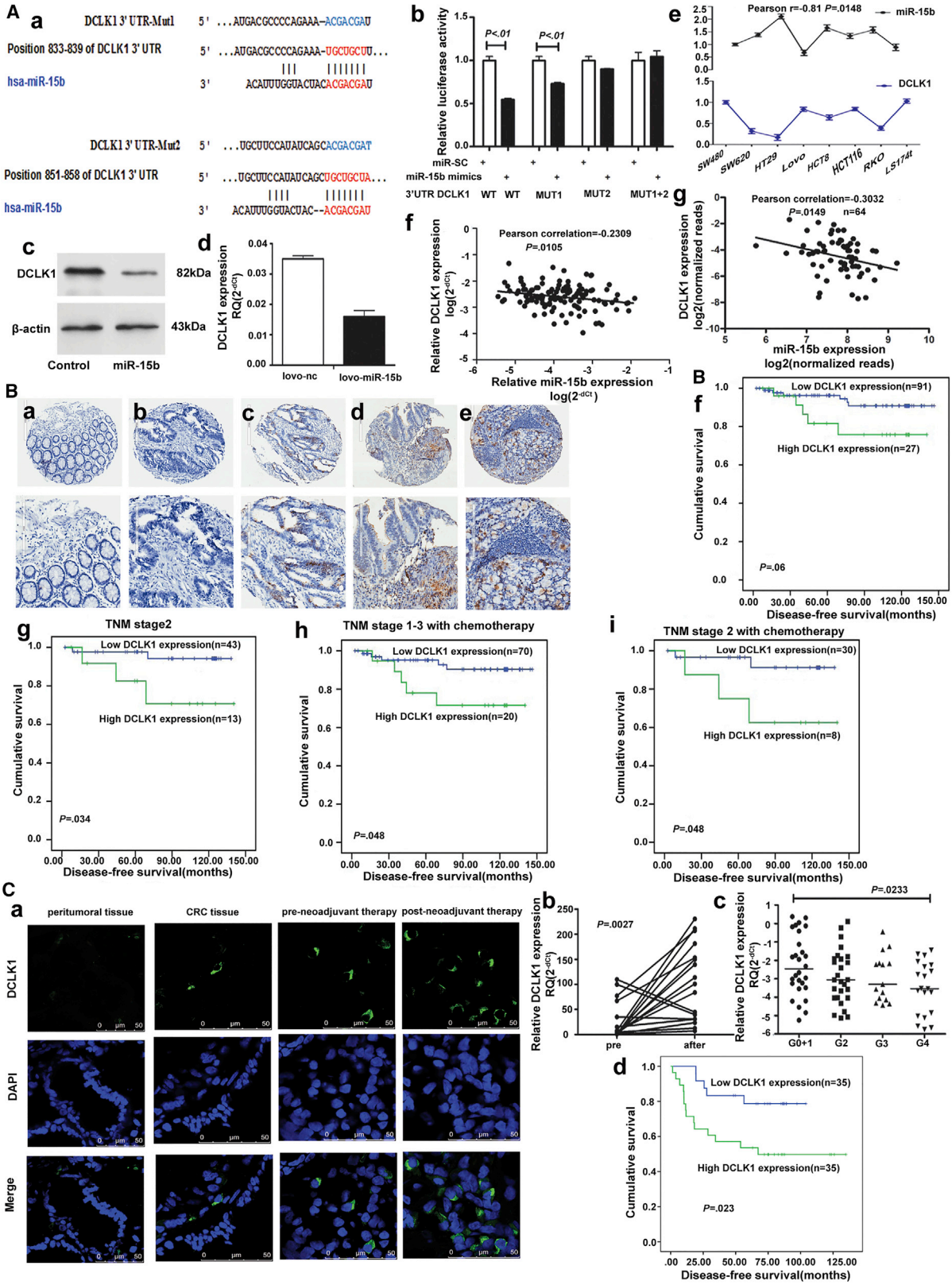

(legend on next page)

be a direct transcriptional target of MYC (Guo et al., 2007; Huang et al., 2011). To further clarify whether DCLK1 could regulate BMI1 expression through a DCLK1 and MYC interaction, exogenous DCLK1 was introduced into Lovo and HCT116 cells to test the level of BMI1. Our results showed that DCLK1 overexpression upregulated BMI1 expression. Conversely, blockage of MYC expression with small interfering RNA decreased the expression of BMI1. Furthermore, MYC interference partially blocked DCLK1-increased BMI1 expression (Figures 5F, b–d, and S5B).

We also examined the levels of MYC and BMI1 in sorted DCLK1+ and DCLK1− HCT116 cells. The expressions of MYC and BMI1 in sorted DCLK1+ CRC cells were higher than in DCLK1− cells. Because MYC is a target molecule of the WNT/β-CATENIN pathway (Li et al., 2015), we further investigated the activity of β-CATENIN pathway in DCLK1+ cells. The levels of CTNNB1 were clearly elevated more in DCLK1+ cells than in DCLK1− cells. The levels of several important CTNNB1 target genes, including CCND1, JUN, and CD44, were upregulated in DCLK1+ cells. Several components of β-CATENIN pathway, such as WNT3A, WNT5A, DVL2, DVL3, and TCF1/TCF7 were upregulated in DCLK1+ cells. Phosphorylation of GSK3β at Ser9, which can be monitored using phosphor-specific antibodies, inhibits its kinase activity (Cross et al., 1995). The phosphorylation of GSK3β at Ser9 in DCLK1+ CRC cells was upregulated whereas the level of GSK3β was downregulated, which was indicative of a decrease in GSK3β activity (Figure S5C).

DISCUSSION

More insightful predictive biomarkers that can predict sensitivity to chemo/radiation are in urgent need to facilitate identification of patients who would actually benefit from chemo/radiation. We report that miR-15b expression may serve as an independent and significant biomarker predicting survival and therapeutic outcome in CRC patients. Hsa-miR-15b expression correlated positively with the sensitivity of CRC to chemo-/radiotherapy. We further demonstrate that miR-15b enhances chemo-/radiotherapy sensitivity of CRC by repressing self-renewal, tumorigenicity, and chemo-/radioresistance of CRC TICs *in vitro* and *in vivo*.

Our study revealed that decreased miR-15b expression correlates significantly with advanced TNM stages and liver metastases in CRC, consistent with published studies supporting miR-15b as a tumor suppressor. Its expression was reported to be negatively correlated with tumor recurrence in liver cancer and gliomas (Chung et al., 2010; Sun et al., 2015), and deletion of miR-15b promoted B-cell malignancies (Lovat et al., 2015), besides, miR-15 and miR-16 induced apoptosis and modulated multi-drug resistance by targeting BCL2 in chronic lymphocytic leukemia and gastric cancer (Cimmino et al., 2005; Xia et al., 2008). However, the exact roles of miR-15b in CRC remain elusive. Our results are compatible with the report by Aslam et al (2015), which stated that expression of miR-15b was significantly downregulated in "high-risk B" tumors compared with Dukes A, "low-risk B" or C without metastasis in CRC. However, different groups reported that miR-15b could promote

Figure 3. DCLK1 Is Target of miR-15b and Negatively Correlated with Prognosis of CRC Treated with Chemo-/Radiotherapy

(A) (a) Schematic illustration of the predicted miR-15b-binding sites in *DCLK1* 3′-UTR; (b) luciferase reporter assay shows miR-15b inhibited the wild-type rather than the mutant, and 3′-UTRs of *DCLK1* reporter activities strongly. The data represent the mean ± SD of three independent experiments with quadruplicate samples. Student's t test, $p < 0.01$ versus control (wild-type 3′ -UTR reporter vector + miR scramble) or mutant 3′-UTR reporter group (mutant 3′-UTR reporter + miR-15b mimics/miR scramble); (c) western blot results show the proteins of DCLK1 in lovo cells following lenti-pre-15b infection. Data refer to a representative experiment out of three, which gave similar results. (d) *DCLK1* mRNA levels were suppressed in overexpressing miR-15b lovo cells; Data are from the mean of three independent experiments ± SE. (e) The inverse correlation of miR-15b against *DCLK1* mRNA expression was determined in indicated cells. (f and g) The significant reverse correlation between miR-15b expression and *DCLK1* mRNA levels in CRC samples (122 cases from cohort 1 and 64 cases from TCGA database, using two-tailed Pearson's test).

(B) Expression patterns of *DCLK1* RNAscope in tissue microarrays of cohort 2. The expression of *DCLK1* mRNA in adjacent non-malignant mucosa (a), and CRC tissues with negative (b), low (c), moderate (d), and high (e) DCLK1 mRNA expression. Positive cells are stained brown. Scale bars, 300 μm (up), 200 μm (below). (f–i) Kaplan-Meier analysis of the correlation between *DCLK1* expression and tumor recurrence or chemotherapy outcome in patients with CRC in cohort 2.

(C) *DCLK1* expression in paired specimens obtained pre and after neoadjuvant radiotherapy by fluorescence immunohistochemistry (a, scale bars, 50 μm) or qRT-PCR (b, Wilcoxon matched pairs test). (c) Association between *DCLK1* expression in pretreatment biopsy tissue samples and TRG in 92 LARC patients (from cohort 3) who received nRT by qRT-PCR, Mann-Whitney test. (d) Kaplan-Meier analysis of the correlation between *DCLK1* expression in post-nRT rectal cancer and tumor recurrence in 70 LARC patients (cohort 4).

In (B, f, g, h, and i), *DCLK1* positive expression was defined as high expression; *DCLK1* negative expression was defined as low expression. In (C, d), the patients were divided into two groups according to the median expression value. $p \leq 0.05$ was considered statistically significant. See also Figure S5.

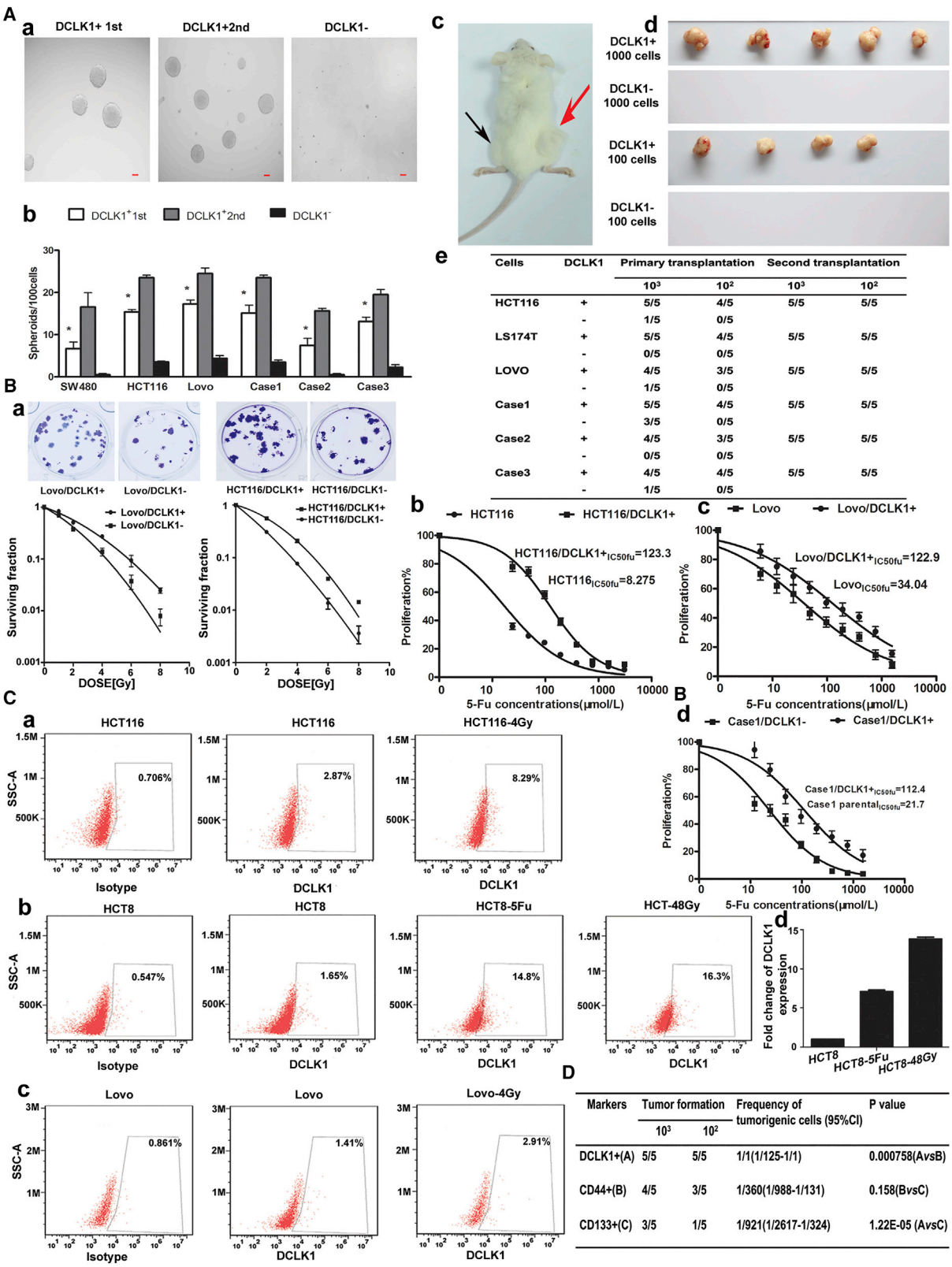

Cells	DCLK1	Primary transplantation		Second transplantation	
		10^3	10^2	10^3	10^2
HCT116	+	5/5	4/5	5/5	5/5
	-	1/5	0/5		
LS174T	+	5/5	4/5	5/5	5/5
	-	0/5	0/5		
LOVO	+	4/5	3/5	5/5	5/5
	-	1/5	0/5		
Case1	+	5/5	4/5	5/5	5/5
	-	3/5	0/5		
Case2	+	4/5	3/5	5/5	5/5
	-	0/5	0/5		
Case3	+	4/5	4/5	5/5	5/5
	-	1/5	0/5		

D

Markers	Tumor formation		Frequency of tumorigenic cells (95%CI)	P value
	10^3	10^2		
DCLK1+(A)	5/5	5/5	1/1(1/125-1/1)	0.000758(AvsB)
CD44+(B)	4/5	3/5	1/360(1/988-1/131)	0.158(BvsC)
CD133+(C)	3/5	1/5	1/921(1/2617-1/324)	1.22E-05 (AvsC)

(legend on next page)

epithelial-mesenchymal transition (EMT) and tumor metastasis in pancreatic cancer, as well as inhibit apoptosis and correlate with poor prognosis in malignant melanoma (Satzger et al., 2010; Zhang et al., 2015), reflecting the complexity of regulation and functions of miRs in the context of different tumors.

We also detected an association between miR-15b expression levels and the prognosis or therapeutic outcome of CRC. In both cohorts the association was independent of other clinical covariates, indicating that miR-15b expression may be a useful prognostic biomarker to help identify patients with poor prognosis. Moreover, patients who responded to 5-FU-based therapy harbor higher expression levels of miR-15b than patients who did not respond to the treatment. Given the widespread use of 5-FU-based therapy in the management of CRC, our results may assist in identifying patients with a higher likelihood of responding to this agent.

In two other cohorts, we demonstrated that miR-15b expression positively correlated with the sensitivity to neoadjuvant radiotherapy in rectal cancer patients. High miR-15b expression in pretreatment tumor biopsies was associated with a higher TRG score after nRT. MiR-15b expression in post-nRT rectal tumor tissues correlates with prognosis in LARC patients. LARC patients with high levels of miR-15b expression were found to have better DFS. Therefore, our findings support that miR-15b may serve as a predictive biomarker for the efficacy of nRT in patients with rectal cancer.

We next investigated the effects of miR-15b on CRC development, progression, and sensitivity to chemo-/radiotherapy by both *in vitro* and *in vivo* assays. Our results support the hypothesis that miR-15b plays an important role during tumorigenesis and chemo-/radioresistance in CRC.

We further investigated the signaling pathways underlying miR-15b-mediated effects. Through an integrated analysis of software predictions, expression correlation, and functional studies, we identified *DCLK1* as a functional downstream target of miR-15b. DCLK1 is a microtubule-associated protein in post-mitotic neurons, with a C-terminal serine/threonine kinase domain consisting of a calcium calmodulin kinase, which is able to regulate a variety of protein interactions. Research studies showed that DCLK1 is implicated in CNS development and modulates speech and cognitive functions (Lin et al., 2000). Notably, DCLK1 was identified as a putative gastrointestinal stem cell marker (May et al., 2008). DCLK1 was reported to be associated with poor prognosis in CRC patients, its expression in Barrett esophagitis was significantly higher than normal esophagus tissue, and its increased expression induced EMT in pancreatic adenocarcinoma (Gagliardi et al., 2012; Sureban et al., 2011; Vega et al., 2012). Nakanishi et al. (2013) identified DCLK1 as a colorectal tumor but not normal intestinal stem cell marker, and DCLK1+ CRC cells HCT116 and SW480 displayed TIC properties *in vitro* (Li and Bellows, 2013).

Our current study demonstrates that high DCLK1 expression is associated with poor therapeutic outcome of CRC patients and plays an important role in CRC TIC properties, including tumor initiation, self-renewal, and resistance to 5-FU and radiotherapy. We identify DCLK1 as a biomarker of CRC TICs from freshly resected tumor specimens. Significant miR-15b downregulation was observed in DCLK1+ CRC tissues and sorted CRC cells, and overexpression of miR-15b reversed functions of CRC TICs, as exhibited by suppressed self-renewal and tumorigenic properties as well as restored chemo-/radiosensitivity in the DCLK1+TICs.

Furthermore, we also demonstrated that BMI1 might be a potential downstream target of miR-15b-DCLK1 signaling cascades. Interestingly, BMI1 was reported to be a direct target of miR-15b and reduced miR-15b expression was

Figure 4. DCLK1 Expression Drives the TIC Phenotype and Chemo-/Radiotherapy Resistance

(A) (a) Phase contrast micrographs demonstrate that FACS-sorted DCLK1+ HCT116 cells can form primary (first) and serially passaged (second) spheroids easily. Data refer to a representative experiment out of three, which gave similar results. Scale bars, 50 μm. (b) Histograms show different spheroid formation efficiency of the DCLK1+ cells and DCLK1− cells from indicated sources. Bars are the mean ± SD of three independent experiments (n = 5). *Student's t test. (c) Photograph showing tumor formation in NOD SCID mice (red arrow, tumor growth of DCLK1+ cell population; black arrow, no tumor growth of DCLK1− cells). (d) The dissected tumors formed with sorted DCLK1+ HCT116 cells. Five mice/group were transplanted. (e) Tumor formation of serial transplantation assay of DCLK1+ and DCLK1− subpopulations in NOD SCID mice.

(B) (a) The clonogenic survival of DCLK1+ and DCLK1− cells sorted from HCT116 and lovo cells. Data refer to a representative experiment out of three, which gave similar results. (b–d) The IC_{50} of 5-FU in DCLK1+ and DCLK1− cells sorted from HCT116, lovo, and case1 cells. Data are from the mean of three independent experiments ± SE.

(C) Flow cytometry measured the frequencies of DCLK1+ cells in HCT116 (a) and lovo (c) cells after 4 Gy irradiation. The frequencies of DCLK1+ cells in 5-FU/radioresistant HCT8 cells (b). Data refer to a representative experiment out of three, which gave similar results. qRT-PCR assayed the expression of *DCLK1* mRNA in HCT8 and 5-FU/radioresistant HCT8 (d). Data are from the mean of three independent experiments ± SE.

(D) Tumorigenic cell frequency in each fraction of HCT116 cells was determined with limiting dilution assay in NOD SCID mice.

$p \leq 0.05$ was considered statistically significant. See also Figure S4.

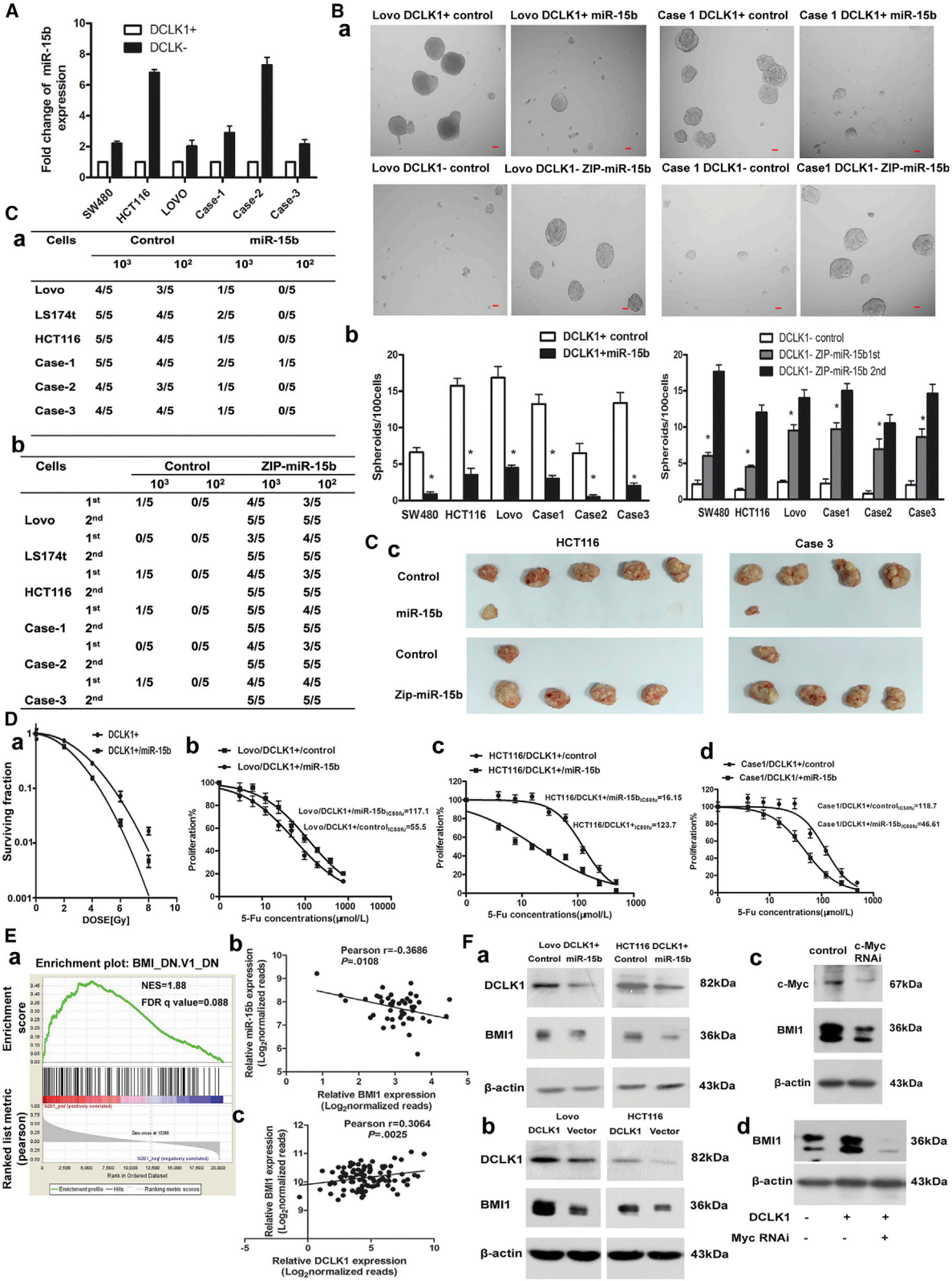

Cells	Control		miR-15b	
	10^3	10^2	10^3	10^2
Lovo	4/5	3/5	1/5	0/5
LS174t	5/5	4/5	2/5	0/5
HCT116	5/5	4/5	1/5	0/5
Case-1	5/5	4/5	2/5	1/5
Case-2	4/5	3/5	1/5	0/5
Case-3	4/5	4/5	1/5	0/5

Cells		Control		ZIP-miR-15b	
		10^3	10^2	10^3	10^2
Lovo	1st	1/5	0/5	4/5	3/5
	2nd			5/5	5/5
LS174t	1st	0/5	0/5	3/5	4/5
	2nd			5/5	5/5
HCT116	1st	1/5	0/5	4/5	3/5
	2nd			5/5	5/5
Case-1	1st	1/5	0/5	5/5	4/5
	2nd			5/5	5/5
Case-2	1st	0/5	0/5	4/5	3/5
	2nd			5/5	5/5
Case-3	1st	1/5	0/5	4/5	4/5
	2nd			5/5	5/5

(legend on next page)

associated with chemotherapeutic resistance in tongue squamous cell carcinomas with poor patient survival (Sun et al., 2012). These results advocate that miR-15b may downregulate BMI1 signaling by either inhibiting DCLK1/MYC interaction or directly targeting BMI1, leading to subsequent suppression of TIC functions. MYC is a target molecule of WNT/β-CATENIN pathway (Li et al., 2015) and the MYC-driven epigenetic reprogramming favors the formation and maintenance of TICs (Poli et al., 2018). Growing evidence shows that WNT/β-CATENIN signaling is highly active in TICs and may have a role in CRC TICs self-renewal (Vermeulen et al., 2010). Upon WNT activation or genetic mutations of WNT components, β-CATENIN accumulates in the cytoplasm and then translocates into the nucleus. Consequently, it binds to LEF-1/TCF4 and some other co-regulators to promote the transcription of target genes such as *JUN, MYC,* and *CCND1*(Zhan et al., 2017). In sorted DCLK1+ TICs, WNT/β-CATENIN signaling is highly active in DCLK1+ CRC cells and DCLK1 might regulate MYC expression through β-CATENIN pathway. Taken together, our results indicate that miR-15b may influence the efficiency of chemo-/radiotherapy by impeding the crucial functions of TICs through regulating the DCLK1/MYC/BMI1 signaling pathway.

A recent study showed that miR-15a could inhibit CRC cell proliferation and resistance to 5-Fu. YAP1 and DCLK1 were validated to be targets of miR-15a (Fesler et al., 2018). Their results were similar with ours. Both miR-15a and miR-15b belong to the miR-15 family. MiR-15a locates in chromosome 13 (13q14) in human and resides in the intron of a gene of a long noncoding RNA named Dleu2 and is regulated by its promoter (Lerner et al., 2009). MiR-15b locates in chromosome 3 and resides in the intron of a protein-coding gene *SMC4*. MiR-15a-5p and miR-15b-5p are different in four nucleotides, none of them are in the seed sequence, so they may also share a large number of target genes. The seed sequences of miR-15a-3p and miR-15b-3p are quite different, which may contribute more to the different functions of these two microRNA (Huang et al., 2015). We also analyzed the correlation between miR-15a and miR-15b expressions and found a significant positive correlation (Figure S5D).

In conclusion, our results demonstrate that miR-15b could serve as a useful biomarker for prognosis and therapeutic outcome, as well as a candidate therapeutic target to overcome chemo-/radioresistance by suppressing functions of CRC TICs, thereby improving therapeutic efficacy and survival in CRC patients.

EXPERIMENTAL PROCEDURES

Patients and Samples

Cohorts 1 and 2 consisted of 429 I-IV CRC patients without preoperative chemotherapy or radiotherapy. Cohort 3 and 4 consisted of 366 LARC patients with preoperative radiotherapy. A summary of the clinical characteristics of these patients is shown in Tables S1–S3.

Some primary CRC tissues were minced and dissociated into single cells by using the human Tumor Dissociation Kit (Miltenyi Biotec, 130-095-929) according to the manufacturer's instructions for TIC isolation, or xenografted into NOD SCID mice.

Samples collection and usage in the present study were approved by the Ethics Review Committees of Peking University Cancer Hospital and Institute. The details of these cohorts are described in Supplemental Experimental Procedures.

Assessment of Treatment Response and Tumor Downstaging

The seventh edition of the American Joint Committee on Cancer TNM system was used for pathological staging (Edge, 2010). The nRT effect was evaluated using the TRG system by Dworak et al. (1997). The detail of evaluation is described in Supplemental Experimental Procedures.

Figure 5. Expression of miR-15b Reverses Self-Renewal, Tumorigenicity and Chemo-/Radioresistance in DCLK1+ CRC TICs

(A–C) (A) The expression of miR-15b in DCLK1+ and DCLK1− cells were detected using qRT-PCR. Data are from the mean of three independent experiments ± SE. FACS-sorted DCLK1+/− fractions were incubated with pre-miR-15b/ZIP-miR-15b lentiviruses for 2 hr. Some were plated in 96-well plates at 100 cells/well (n = 5) to assay their spheroid formation efficiency and subsequent expansion ability (B, a–b), Scale bars, 50 μm. Data are from the mean of three independent experiments ± SE. Student's t test, $p \leq 0.05$ was considered statistically significant. The others were transplanted into NOD SCID mice (n = 5) to test their tumorigenicity and subsequent expansion ability (C, a–c).

(D) (a) The clonogenic survival of DCLK1+ and miR-15b overexpressing DCLK1+ HCT116 cells. (b–d) The IC_{50} of 5-FU in DCLK1+ and miR-15b overexpressing DCLK1+ HCT116, lovo, and case1 cells. Data are from the mean of three independent experiments ± SE.

(E) (a) DCLK1 associated with the BMI signaling pathway in the GSEA of TCGA CRC dataset. (b and c) Pearson correlation analysis of 53 CRC cases (expression levels of miR-15b and *BMI1*) and 95 CRC cases (expression levels of *DCLK1* and *BMI1*) both from TCGA database. $p \leq 0.05$ was considered statistically significant.

(F) (a) Western blot analysis of DCLK1 and BMI1 expression in DCLK1+ cells from lovo and HCT116 cells after overexpressing miR-15b. (b) DCLK1 and BMI1 expression in lovo and HCT116 cells after overexpressing DCLK1. (c) MYC and BMI1 expression in HCT116 c-MYC-knockdown cells. (d) BMI1 expression in DCLK1 overexpressing HCT116 cells after MYC knockdown.

Data refer to a representative experiment out of three, which gave similar results. See also Figure S5.

Experimental Animals

Male and female NOD SCID (NOD.CB17-prkdcscid/NcrCrl) mice (4–6 weeks old) were purchased from Beijing Vitalriver Experimental Animal Technology Co. Ltd. (Beijing, China). Mice were maintained in a pathogen-free facility and used in accordance with the institutional guidelines for animal care.

Cell Lines

Human CRC cell lines HCT116, HCT8, LS174T, and Lovo were purchased from American Type Culture Collection and were maintained in Dulbecco's Modified Eagle medium (Gibco, Carlsbad, CA) with 10% fetal bovine serum, 100 U/mL penicillin sodium and 100 mg/mL streptomycin sulfate in humidified 5% CO_2 at 37°C. The cell lines have been tested and authenticated (STR [short tandem repeat]) profiling. Chemoresistant cells HCT8-5Fu were established by stepwise exposure of HCT8 cells to increasing concentrations of 5-Fu. Radioresistant cells HCT8-48Gy were generated by sequential irradiation and recovery (Souchek et al., 2014). The detail of generation of radioresistant cell lines is described in Supplemental Experimental Procedures.

Quantitative Real-Time RT-PCR

The details of RNA extraction and quantitative real-time RT-PCR are described in Supplemental Experimental Procedures and all primers are listed in Table S4.

miR-15b *In Situ* Hybridization Analysis

In situ hybridization of microRNAs was performed according to the miRCURY LNA microRNA ISH protocol for formalin-fixed paraffin-embedded tissue. The details of hybridization are described in Supplemental Experimental Procedures and the sequence and hybridization temperature of probes are shown in Table S4.

DCLK1 RNA *In Situ* Hybridization

ISH for DCLK1 was performed with the RNAscope FFPE assay kit (Advanced Cell Diagnostics, Inc., Hayward, CA, USA) according to the manufacturer's instructions. Details of experiments are described in the Supplementary Experimental Procedures.

Oligonucleotide, Lentiviral Vector Construction, and Cell Infection

Mimics of microRNA, microRNA inhibitor, and negative control microRNA oligonucleotides with miR-15b were from RiboBio Co. Ltd (Guangzhou, China).

Lentiviral constructs expressing pre-miR-15b (Lenti-based microRNA precursor constructs; System Biosciences) or anti-miR-15b (miRZips lentiviral-based anti-microRNAs; System Biosciences) were packaged using the pPACKH1 lentivector packaging kit (System Biosciences) in 293TN cells. Details of cell infection are described in the Supplementary Experimental Procedures.

In Vitro Cell Growth, Spreading, Motility, and Invasion Assays

Cell growth was assessed using CCK-8 (Dojindo, Tokyo, Japan) according to the manufacturer's instructions. Cell spreading was evaluated by a wound healing assay. Wound closure was observed by taking time elapsed micro-photos at 0 and 24 hr after scratching. Cell motility or invasion was measured using a Boyden chamber assay with or without Matrigel. Photographs of three randomly selected fields of the fixed cells were taken and cells were counted. Experiments were repeated three times independently. These assays were carried out as previously described (Kong et al., 2012).

In Vivo Tumor Growth and Metastasis Assay

The detail of tumorigenicity study is described in Supplemental Experimental Procedures. All animal experiments were reviewed and approved by the Ethics Review Committee at the Peking University Cancer Hospital.

Luciferase Reporter Assay

The 3′-UTR of *DCLK1* was amplified via PCR from human genomic DNA constructed and cloned into pmiR-RB-REPORT Luciferase, downstream of the firefly luciferase gene to form pMIR-3′-UTR DCLK1, pMIR-3′-UTR DCLK1-Mut1, pMIR-3′-UTR DCLK1-Mut2 and pMIR-3′-UTR *DCLK1* Mut1and 2 constructs (primers are listed in Table S4). Details of experiments are described in the Supplementary Experimental Procedures.

Immunofluorescent Staining and Flow Cytometry Analysis

Cells were detached from culture by 0.02% EDTA/PBS or were dissociated from primary or xenografted tumors by mechanical homogenization, and were stained by mouse anti-CD44 or CD133 monoclonal antibody (1:11 dilution, Miltenyi Biotec, 130-098-110, 130-098-046), rabbit anti-DCLK1 polyclonal antibody (1:33 dilution, Abcam, #ab37994), which were pre-labeled using the Lightning-Link PE-Cy5 Labeling Kit (Innova Biosciences Ltd, Cambridge, UK) at 4°C for 30 min. Labeled samples were analyzed or sorted on a FACSAria II flow cytometer (BD Biosciences, San Jose, CA).

Spheroid Formation Assay

The detail of spheroid formation assay is described in Supplemental Experimental Procedures.

Tumorigenicity Assay

Cells were suspended in 50 μL of plain RPMI1640 and Matrigel (BD Biosciences) mix (1:1) and transplanted s.c. into the armpit of 4- to 6-week-old NOD/SCID male and female mice (5 mice/group, random group). Tumor formation was monitored weekly.

Cell Cytotoxicity Assay

5-FU was obtained from Sigma and was dissolved according to the manufacturer's instructions. The detail of cell cytotoxicity assay is described in Supplemental Experimental Procedures.

Clonogenic Survival Assay

The clonogenic assay was done on single cell suspension as described previously (Rodel et al., 2003). The detail of assay is described in Supplemental Experimental Procedures.

Western Blot Analysis

The following primary antibodies were used with the protocol described in Supplemental Experimental Procedures: rabbit polyclonal anti-human DCLK1, rabbit monoclonal anti-human BMI1 (#ab37994, #ab126783; Abcam, Cambridge, MA), mouse monoclonal anti-human CD44, rabbit monoclonal anti-human Cyclin D1, c-Jun, Wnt3a, Wnt5a, DVL2, DVL3, GSK3β, phosphorylated GSK3β, TCF1/TCF7, β-catenin, GAPDH (#3570, #2978, #9165, #2721, #2530, #3224, #3218, #12456, #5558, #2203, #8480, #5174; Cell Signaling Technology, Beverly, MA) and mouse anti-human c-Myc (sc-40, Santa Cruz Biotechnology).

TCGA Dataset

Details of the analysis of TCGA microRNA-seq, mRNA-seq, and DNA methylation chip dataset are described in Supplemental Experimental Procedures.

Gene Set Enrichment Analysis

GSEA is a computational method of analyzing and interpreting microarray and such data using biological knowledge (Subramanian et al., 2007). The detail of GSEA is described in Supplemental Experimental Procedures.

Statistical Analysis

All data are presented as the mean ± SE and were analyzed using the statistical package SPSS19.0. Data are expressed as median values (interquartile range) in tables or as means ±SE in the figures. Comparisons were performed using the nonparametric Mann-Whitney U test or Kruskal-Wallis test for continuous variables. Spearman's rho correlation test (two-tailed) was used to estimate the correlation between the expression in CRC tissue of each marker and clinical-pathological variables. Survival curves were plotted using the Kaplan-Meier analysis and the log rank test was used to examine significant differences. For the ISH assay, miR-15b or *DCLK1*-positive expression was defined as high expression; miR-15b or *DCLK1* negative expression was defined as low expression. For qRT-PCR analyses, the patients were divided into two groups according to the median expression value. Cox univariate and multivariate proportional hazard models were used to estimate the hazard ratio for each marker. Tumorigenic cell frequency was calculated based on extreme limiting dilution analysis using the web tool at http://bioinf.wehi.edu.au/software/elda/(Hu and Smyth, 2009). $p \leq 0.05$ was considered statistically significant.

SUPPLEMENTAL INFORMATION

Supplemental Information includes Supplemental Experimental Procedures, five figures, and four tables and can be found with this article online at https://doi.org/10.1016/j.stemcr.2018.10.015.

AUTHOR CONTRIBUTIONS

J.G. contributed to study design and data analysis and interpretation, and important intellectual content. D.J., T.Z., and M.L. contributed to study supervision, analysis and interpretation of data, and drafting of the manuscript. Y.Y., J.J., H.Y., M.Q., J.X., Z.Z., H.D., C.S., and Y.H. contributed to data collection and analysis, All authors contributed to writing, critical review, and final approval to submit the paper for publication.

ACKNOWLEDGMENTS

The authors would like to thank Dr Bin Dong, the Department of Pathology, Peking University Cancer Hospital & Institute for her technical assistance. This work was supported by the National Natural Science Foundation (81772565, 81372593, 81201965), Beijing Natural Science Foundation (7132052), and the National High Technology Research and Development Program of China (863 Program) (No.2012AA02A506, 2014AA020801).

Received: March 26, 2018
Revised: October 16, 2018
Accepted: October 17, 2018
Published: November 15, 2018

REFERENCES

Aklilu, M., and Eng, C. (2011). The current landscape of locally advanced rectal cancer. Nat. Rev. Clin. Oncol. *8*, 649–659.

Aslam, M.I., Venkatesh, J., Jameson, J.S., West, K., Pringle, J.H., and Singh, B. (2015). Identification of high-risk Dukes B colorectal cancer by microRNA expression profiling: a preliminary study. Colorectal Dis. *17*, 578–588.

Asuthkar, S., Velpula, K.K., Chetty, C., Gorantla, B., and Rao, J.S. (2012). Epigenetic regulation of miRNA-211 by MMP-9 governs glioma cell apoptosis, chemosensitivity and radiosensitivity. Oncotarget *3*, 1439–1454.

Avoranta, S.T., Korkeila, E.A., Ristamaki, R.H., Syrjanen, K.J., Carpen, O.M., Pyrhonen, S.O., and Sundstrom, J.T. (2013). ALDH1 expression indicates chemotherapy resistance and poor outcome in node-negative rectal cancer. Hum. Pathol. *44*, 966–974.

Bitarte, N., Bandres, E., Boni, V., Zarate, R., Rodriguez, J., Gonzalez-Huarriz, M., Lopez, I., Javier Sola, J., Alonso, M.M., Fortes, P., et al. (2011). MicroRNA-451 is involved in the self-renewal, tumorigenicity, and chemoresistance of colorectal cancer stem cells. Stem Cells *29*, 1661–1671.

Calin, G.A., and Croce, C.M. (2006). MicroRNA signatures in human cancers. Nat. Rev. Cancer *6*, 857–866.

Cho, Y.M., Kim, Y.S., Kang, M.J., Farrar, W.L., and Hurt, E.M. (2012). Long-term recovery of irradiated prostate cancer increases cancer stem cells. Prostate *72*, 1746–1756.

Chung, G.E., Yoon, J.H., Myung, S.J., Lee, J.H., Lee, S.H., Lee, S.M., Kim, S.J., Hwang, S.Y., Lee, H.S., and Kim, C.Y. (2010). High expression of microRNA-15b predicts a low risk of tumor recurrence following curative resection of hepatocellular carcinoma. Oncol. Rep. *23*, 113–119.

Cimmino, A., Calin, G.A., Fabbri, M., Iorio, M.V., Ferracin, M., Shimizu, M., Wojcik, S.E., Aqeilan, R.I., Zupo, S., Dono, M., et al. (2005). miR-15 and miR-16 induce apoptosis by targeting BCL2. Proc. Natl. Acad. Sci. U S A *102*, 13944–13949.

Cross, D.A., Alessi, D.R., Cohen, P., Andjelkovich, M., and Hemmings, B.A. (1995). Inhibition of glycogen synthase kinase-3 by insulin mediated by protein kinase B. Nature *378*, 785–789.

Dworak, O., Keilholz, L., and Hoffmann, A. (1997). Pathological features of rectal cancer after preoperative radiochemotherapy. Int. J. Colorectal Dis. *12*, 19–23.

Eaton, C.L., Colombel, M., van der Pluijm, G., Cecchini, M., Wetterwald, A., Lippitt, J., Rehman, I., Hamdy, F., and Thalman, G. (2010). Evaluation of the frequency of putative prostate cancer stem cells in primary and metastatic prostate cancer. Prostate *70*, 875–882.

S. Edge, D.R. Byrd, C.C. Compton, A.G. Fritz, F. Greene, and A. Trotti, eds. (2010). AJCC Cancer Staging Manual, Seventh Edition (Springer-Verlag).

Fesler, A., Liu, H., and Ju, J. (2018). Modified miR-15a has therapeutic potential for improving treatment of advanced stage colorectal cancer through inhibition of BCL2, BMI1, YAP1 and DCLK1. Oncotarget *9*, 2367–2383.

Gagliardi, G., Goswami, M., Passera, R., and Bellows, C.F. (2012). DCLK1 immunoreactivity in colorectal neoplasia. Clin. Exp. Gastroenterol. *5*, 35–42.

Gangadhar, T., and Schilsky, R.L. (2010). Molecular markers to individualize adjuvant therapy for colon cancer. Nat. Rev. Clin. Oncol. *7*, 318–325.

Grady, W.M., and Tewari, M. (2010). The next thing in prognostic molecular markers: microRNA signatures of cancer. Gut *59*, 706–708.

Guo, W.J., Datta, S., Band, V., and Dimri, G.P. (2007). Mel-18, a polycomb group protein, regulates cell proliferation and senescence via transcriptional repression of Bmi-1 and c-Myc oncoproteins. Mol. Biol. Cell *18*, 536–546.

Hu, Y., and Smyth, G.K. (2009). ELDA: extreme limiting dilution analysis for comparing depleted and enriched populations in stem cell and other assays. J. Immunol. Methods *347*, 70–78.

Huang, R., Cheung, N.K., Vider, J., Cheung, I.Y., Gerald, W.L., Tickoo, S.K., Holland, E.C., and Blasberg, R.G. (2011). MYCN and MYC regulate tumor proliferation and tumorigenesis directly through BMI1 in human neuroblastomas. FASEB J. *25*, 4138–4149.

Huang, E., Liu, R., and Chu, Y. (2015). miRNA-15a/16: as tumor suppressors and more. Future Oncol. *11*, 2351–2363.

Ji, D., Chen, Z., Li, M., Zhan, T., Yao, Y., Zhang, Z., Xi, J., Yan, L., and Gu, J. (2014). MicroRNA-181a promotes tumor growth and liver metastasis in colorectal cancer by targeting the tumor suppressor WIF-1. Mol. Cancer *13*, 86.

Kong, K.L., Kwong, D.L., Chan, T.H., Law, S.Y., Chen, L., Li, Y., Qin, Y.R., and Guan, X.Y. (2012). MicroRNA-375 inhibits tumour growth and metastasis in oesophageal squamous cell carcinoma through repressing insulin-like growth factor 1 receptor. Gut *61*, 33–42.

Kuhn, N.Z., and Tuan, R.S. (2010). Regulation of stemness and stem cell niche of mesenchymal stem cells: implications in tumorigenesis and metastasis. J. Cell. Physiol. *222*, 268–277.

Lerner, M., Harada, M., Loven, J., Castro, J., Davis, Z., Oscier, D., Henriksson, M., Sangfelt, O., Grander, D., and Corcoran, M.M. (2009). DLEU2, frequently deleted in malignancy, functions as a critical host gene of the cell cycle inhibitory microRNAs miR-15a and miR-16-1. Exp. Cell Res. *315*, 2941–2952.

Li, L., and Bellows, C.F. (2013). Doublecortin-like kinase 1 exhibits cancer stem cell-like characteristics in a human colon cancer cell line. Chin. J. Cancer Res. *25*, 134–142.

Li, X., Bai, B., Liu, L., Ma, P., Kong, L., Yan, J., Zhang, J., Ye, Z., Zhou, H., Mao, B., et al. (2015). Novel beta-carbolines against colorectal cancer cell growth via inhibition of Wnt/beta-catenin signaling. Cell Death Discov. *1*, 15033.

Lin, P.T., Gleeson, J.G., Corbo, J.C., Flanagan, L., and Walsh, C.A. (2000). DCAMKL1 encodes a protein kinase with homology to doublecortin that regulates microtubule polymerization. J. Neurosci. *20*, 9152–9161.

Lopes-Ramos, C.M., Habr-Gama, A., Quevedo Bde, S., Felicio, N.M., Bettoni, F., Koyama, F.C., Asprino, P.F., Galante, P.A., Gama-Rodrigues, J., Camargo, A.A., et al. (2014). Overexpression of miR-21-5p as a predictive marker for complete tumor regression to neoadjuvant chemoradiotherapy in rectal cancer patients. BMC Med. Genomics *7*, 68.

Lovat, F., Fassan, M., Gasparini, P., Rizzotto, L., Cascione, L., Pizzi, M., Vicentini, C., Balatti, V., Palmieri, D., Costinean, S., et al. (2015). miR-15b/16-2 deletion promotes B-cell malignancies. Proc. Natl. Acad. Sci. U S A *112*, 11636–11641.

May, R., Riehl, T.E., Hunt, C., Sureban, S.M., Anant, S., and Houchen, C.W. (2008). Identification of a novel putative gastrointestinal stem cell and adenoma stem cell marker, doublecortin and CaM kinase-like-1, following radiation injury and in adenomatous polyposis coli/multiple intestinal neoplasia mice. Stem Cells *26*, 630–637.

Nakanishi, Y., Seno, H., Fukuoka, A., Ueo, T., Yamaga, Y., Maruno, T., Nakanishi, N., Kanda, K., Komekado, H., Kawada, M., et al. (2013). Dclk1 distinguishes between tumor and normal stem cells in the intestine. Nat. Genet. *45*, 98–103.

Poli, V., Fagnocchi, L., Fasciani, A., Cherubini, A., Mazzoleni, S., Ferrillo, S., Miluzio, A., Gaudioso, G., Vaira, V., Turdo, A., et al. (2018). MYC-driven epigenetic reprogramming favors the onset of tumorigenesis by inducing a stem cell-like state. Nat. Commun. *9*, 1024.

Rodel, C., Haas, J., Groth, A., Grabenbauer, G.G., Sauer, R., and Rodel, F. (2003). Spontaneous and radiation-induced apoptosis in colorectal carcinoma cells with different intrinsic radiosensitivities: survivin as a radioresistance factor. Int. J. Radiat. Oncol. Biol. Phys. *55*, 1341–1347.

Satzger, I., Mattern, A., Kuettler, U., Weinspach, D., Voelker, B., Kapp, A., and Gutzmer, R. (2010). MicroRNA-15b represents an independent prognostic parameter and is correlated with tumor cell proliferation and apoptosis in malignant melanoma. Int. J. Cancer *126*, 2553–2562.

Siegel, R., Desantis, C., and Jemal, A. (2014). Colorectal cancer statistics, 2014. CA Cancer J. Clin. *64*, 104–117.

Song, B., Wang, Y., Xi, Y., Kudo, K., Bruheim, S., Botchkina, G.I., Gavin, E., Wan, Y., Formentini, A., Kornmann, M., et al. (2009). Mechanism of chemoresistance mediated by miR-140 in human osteosarcoma and colon cancer cells. Oncogene *28*, 4065–4074.

Souchek, J.J., Baine, M.J., Lin, C., Rachagani, S., Gupta, S., Kaur, S., Lester, K., Zheng, D., Chen, S., Smith, L., et al. (2014). Unbiased analysis of pancreatic cancer radiation resistance reveals cholesterol

biosynthesis as a novel target for radiosensitisation. Br. J. Cancer *111*, 1139–1149.

Subramanian, A., Kuehn, H., Gould, J., Tamayo, P., and Mesirov, J.P. (2007). GSEA-P: a desktop application for gene set enrichment analysis. Bioinformatics *23*, 3251–3253.

Sun, L., Yao, Y., Liu, B., Lin, Z., Lin, L., Yang, M., Zhang, W., Chen, W., Pan, C., Liu, Q., et al. (2012). MiR-200b and miR-15b regulate chemotherapy-induced epithelial-mesenchymal transition in human tongue cancer cells by targeting BMI1. Oncogene *31*, 432–445.

Sun, G., Yan, S., Shi, L., Wan, Z., Jiang, N., Li, M., and Guo, J. (2015). Decreased expression of miR-15b in human gliomas is associated with poor prognosis. Cancer Biother. Radiopharm. *30*, 169–173.

Sureban, S.M., May, R., Lightfoot, S.A., Hoskins, A.B., Lerner, M., Brackett, D.J., Postier, R.G., Ramanujam, R., Mohammed, A., Rao, C.V., et al. (2011). DCAMKL-1 regulates epithelial-mesenchymal transition in human pancreatic cells through a miR-200a-dependent mechanism. Cancer Res. *71*, 2328–2338.

Van Schaeybroeck, S., Allen, W.L., Turkington, R.C., and Johnston, P.G. (2011). Implementing prognostic and predictive biomarkers in CRC clinical trials. Nat. Rev. Clin. Oncol. *8*, 222–232.

Vega, K.J., May, R., Sureban, S.M., Lightfoot, S.A., Qu, D., Reed, A., Weygant, N., Ramanujam, R., Souza, R., Madhoun, M., et al. (2012). Identification of the putative intestinal stem cell marker doublecortin and CaM kinase-like-1 in Barrett's esophagus and esophageal adenocarcinoma. J. Gastroenterol. Hepatol. *27*, 773–780.

Vermeulen, L., De Sousa, E.M.F., van der Heijden, M., Cameron, K., de Jong, J.H., Borovski, T., Tuynman, J.B., Todaro, M., Merz, C., Rodermond, H., et al. (2010). Wnt activity defines colon cancer stem cells and is regulated by the microenvironment. Nat. Cell Biol. *12*, 468–476.

Wan, L.Y., Deng, J., Xiang, X.J., Zhang, L., Yu, F., Chen, J., Sun, Z., Feng, M., and Xiong, J.P. (2015). miR-320 enhances the sensitivity of human colon cancer cells to chemoradiotherapy in vitro by targeting FOXM1. Biochem. Biophys. Res. Commun. *457*, 125–132.

Xia, L., Zhang, D., Du, R., Pan, Y., Zhao, L., Sun, S., Hong, L., Liu, J., and Fan, D. (2008). miR-15b and miR-16 modulate multidrug resistance by targeting BCL2 in human gastric cancer cells. Int. J. Cancer *123*, 372–379.

Zhan, T., Rindtorff, N., and Boutros, M. (2017). Wnt signaling in cancer. Oncogene *36*, 1461–1473.

Zhang, W.L., Zhang, J.H., Wu, X.Z., Yan, T., and Lv, W. (2015). miR-15b promotes epithelial-mesenchymal transition by inhibiting SMURF2 in pancreatic cancer. Int. J. Oncol. *47*, 1043–1053.

Zhao, C., Zhao, Q., Zhang, C., Wang, G., Yao, Y., Huang, X., Zhan, F., Zhu, Y., Shi, J., Chen, J., et al. (2017). miR-15b-5p resensitizes colon cancer cells to 5-fluorouracil by promoting apoptosis via the NF-kappaB/XIAP axis. Sci. Rep. *7*, 4194.